UWB Elliptical Monopoles With a Reconfigurable Band Notch Using MEMS Switches Actuated Without Bias Lines

Symeon Nikolaou, *Member, IEEE*, Nickolas D. Kingsley, *Member, IEEE*, George E. Ponchak, *Senior Member, IEEE*, John Papapolymerou, *Senior Member, IEEE*, and Manos M. Tentzeris, *Senior Member, IEEE*

***Abstract*—Two CPW-fed elliptical monopoles were fabricated on liquid crystal polymer (LCP) with reconfigurable rejection band (band-notch) characteristics in the frequency range between 5 and 6 GHz. The first antenna uses a $\lambda/2$ long, U-shaped slot and the second antenna uses two symmetrically placed $\lambda/4$ long, inverted L-shaped stubs as resonating elements. Microelectromechanical system (MEMS) switches are used to activate and deactivate the resonating elements without the need of dc bias lines due to a novel design of the switch geometry. Transmission line models and surface current distributions are used to explain the effect of the added resonating elements. Reflection coefficient radiation pattern and gain measurements are presented to verify the design concepts featuring a very satisfactory performance.**

***Index Terms*—Band-notch, microelectromechanical system (MEMS), reconfigurable, ultrawideband (UWB) .**

I. Introduction

THE rapidly increasing number of wireless applications has led to a very heavy congestion in the available RF and wireless spectrum, causing significant interference among the different users and degrading the performance of the affected radios. To overcome this problem in an opportunistic way, agile radios are required [1] that demand the use of "smart," reconfigurable antennas capable of canceling in-band interference. Since the ultrawideband (UWB) radios share part of the spectrum with the HIPERLAN/2 applications (5.15–5.35 GHz, 5.470–5.725 GHz) and the wireless local area network (WLAN) applications using the IEEE 802.11a (5.15–5.35 GHz, 5.725–5.825 GHz) protocol, an UWB antenna with reconfigurable band-rejection characteristic at the WLAN frequencies is highly desirable.

Several designs of UWB antennas with band rejection characteristics have been investigated and successfully implemented in the past. Two parasitic patches were used in [2], two linear slots were used for the Vivaldi antenna presented in [3] and the printed log-periodic antenna presented in [4], while a split ring resonator (SRR) was added on the microstrip-fed monopole suggested in [5]. However none of those antennas had reconfigurable band-notch characteristics. Some antennas with endogenous band-notch characteristics were also introduced, like the combined $\lambda/4$ monopoles [6], the monopole with the integrated filter [7], the sail-boat antenna presented in [8] and the fractal antenna proposed in [9]. Two open-circuit stubs were used in [10], in an approach similar to one of the two solutions suggested in the present paper. However, the technique that was adopted by most researchers was the integration of a U-shaped slot on a monopole [11]–[14] or the integration of stubs with the monopole [15]. Numerous researchers have integrated microelectromechanical system (MEMS) switches and antennas to develop frequency [16], [17] or radiation pattern [18] reconfigurable antennas. In all those cases, the MEMS switches were actuated using dc bias lines.

In this paper, two UWB monopole antennas with an integrated MEMS switch that can be actuated to place a stopband at the HIPERLAN/2 and WLAN frequencies are demonstrated for the first time. The MEMS switches are designed so that they do not require extra bias lines; the bias is applied to the RF signal line. The lack of bias lines for the MEMS switches in the proposed topologies makes the fabrication easier and improves the radiation performance of the antenna since there is no coupling or leakage from the bias lines. For the first antenna, a U-shaped slot is placed within the monopole and a MEMS switch is used to short the resonant slot when the band rejection is not required. For the second antenna, two inverted L-shaped open circuit stubs are symmetrically placed near the elliptical radiator and MEMS switches connect them to the radiator when the band rejection is required. In the following sections, the antennas design is given first, then their operation and design are confirmed through simulations and experimental characterization.

II. Antenna Design

The UWB antenna used for the integration of the reconfigurable "band-notch rejecting" elements is a CPW-fed elliptical monopole fabricated on 100 μm thick liquid crystal polymer

Manuscript received October 25, 2007; revised July 21, 2008. First published June 05, 2009; current version published August 05, 2009. This work was supported in part by the Army Research Office under Grant W911NF-06-1-0362.

S. Nikolaou is with Frederick University, Nicosia 1036, Cyprus (e-mail: s.nikolaou@frederick.ac.cy; simos.nikolaou@gmail.com).

N. D. Kingsley is with Auriga Measurement Systems, Lowell, MA 01854 USA.

G. E. Ponchak is with the NASA - Glenn Research Center, Cleveland, OH USA.

J. Papapolymerou and M. M. Tentzeris are with the Electrical and Computer Engineering Department, Georgia Institute of Technology, Atlanta, GA 30308 USA.

Color versions of one or more of the figures in this paper are available online at http://ieeexplore.ieee.org.

Digital Object Identifier 10.1109/TAP.2009.2024450

(LCP) ($\varepsilon_r = 3$, $\tan\delta = 0.002$). The LCP samples were polished to reduce the surface roughness and allow for the MEMS switch fabrication.

The elliptical radiator has a major axis $A = 18$ mm and a secondary axis $B = 15.30$ mm. Fig. 1 presents the details of the schematic design and its dimensions are summarized in Table I. The overall width of the antenna, W_{g1}, is 26.88 mm and the ground length is $L_g = 20.7$ mm. A CPW feed line with central conductor width $W_{f2} = 3.89$ mm and ground-signal gap $G_2 = 100$ μm is used, resulting in a characteristic impedance (Z_o) of 50 Ohms. In order to use 850 μm pitch probes for measurements, the CPW line is linearly tapered down to a narrower CPW line with 50 Ohm characteristic impedance ($W_{f1} = 1.28$ mm and $G_1 = 50$ μm) that had length only $L_1 = 1$ mm. A customized transition from the standard CPW line (W_{f2}, G_2) to the ellipse was used to improve the matching. The matching improvement can be seen in Fig. 2 where the input impedance of two antennas, one referred to as "Standard CPW" and one referred to as "Reference" are presented on a Smith chart. The "Standard CPW" does not use any CPW-radiator transition; a standard, uniform width CPW line with the above mentioned geometrical characteristics (W_{f2}, G_2) is terminated with the elliptical radiator. The "Reference" is identical with the antenna presented in Fig. 1 without the slot or the two open stubs. It is referred to as "Reference" because it will be compared to the antennas with the reconfigurable resonating elements. Fig. 2 shows that a uniform CPW line cannot establish good matching for this elliptical monopole, but the use of an appropriate CPW to radiator transition can achieve a SWR less than 2 across the whole UWB range. The two lines represent measurements taken between 2–12 GHz. The segment of the "Reference" line that falls outside the SWR = 2 circle corresponds to the frequency range from 2–3 GHz, which is not part of the UWB frequency range.

Two different approaches (a U-shaped slot and two inverted L-shaped open stubs) are demonstrated to achieve a reconfigurable band notch between 5.2 and 6 GHz. The U-shaped slot is presented in Fig. 1(a). It consists of two parallel segments of length $L_{S1} = 8.8$ mm and a third segment with length $W_{S1} = 5.6$ mm that is positioned $D_1 = 2.6$ mm from the nearest ground edge. In the middle of this third edge and along the symmetry plane of the antenna, a MEMS switch is integrated to selectively short the 0.2 mm wide slot. Another very thin slot (only 3 μm wide) is created parallel to the third segment at a distance $S1 = 0.7$ mm from it. Therefore an isolated rectangular segment is defined which serves as the floating dc ground, which is necessary for the MEMS switch actuation. For the design shown in Fig. 1(b), two inverted L open stubs with width $G_{S2} = 200$ μm and total length 10.41 mm ($L_{S2} + W_{S2} + G_{S2}$) cause the band notch. Both stubs are placed at a distance $D2 = 1.8$ mm from the top point of the ellipse. Two MEMS switches are used to electrically connect and disconnect the two stubs to the elliptical radiator. The switches are positioned 0.4 mm from the ellipse. Bias lines are not needed in neither the slot nor the stubs case for the MEMS switch actuation because of the switch topology [21].

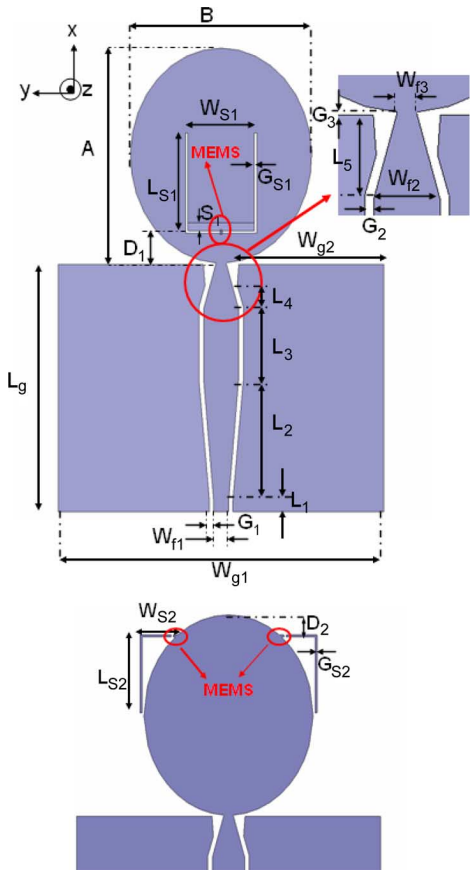

Fig. 1. Antenna schematic (a) U-shaped slot and (b) L-shaped stubs.

TABLE I
ANTENNA SCHEMATIC DIMENSIONS

L_1	1.00 mm	W_{S2}	3.41 mm	W_{f3}	0.85 mm
L_2	10.00 mm	G_{S2}	0.20 mm	S_1	0.70 mm
L_3	6.00 mm	L_{S2}	6.80 mm	G_1	0.05 mm
L_4	1.93 mm	D_2	1.80 mm	G_2	0.10 mm
L_5	3.70 mm	W_{g1}	26.88 mm	G_3	0.11 mm
W_{S1}	5.60 mm	W_{g2}	12.25mm	L_g	20.70 mm
G_{S1}	0.20 mm	W_{f1}	1.28 mm	A	18.00 mm
L_{S1}	8.8 mm	W_{f2}	2.97 mm	B	15.30 mm
D_1	2.60 mm				

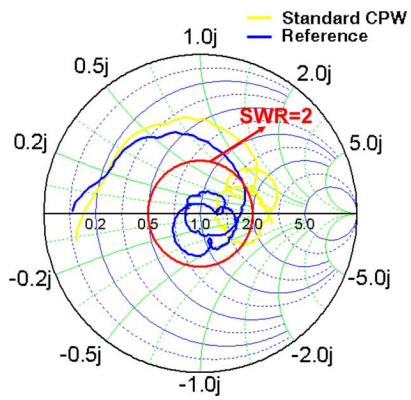

Fig. 2. Input impedance for "Standard CPW" and "Reference" antennas on Smith chart.

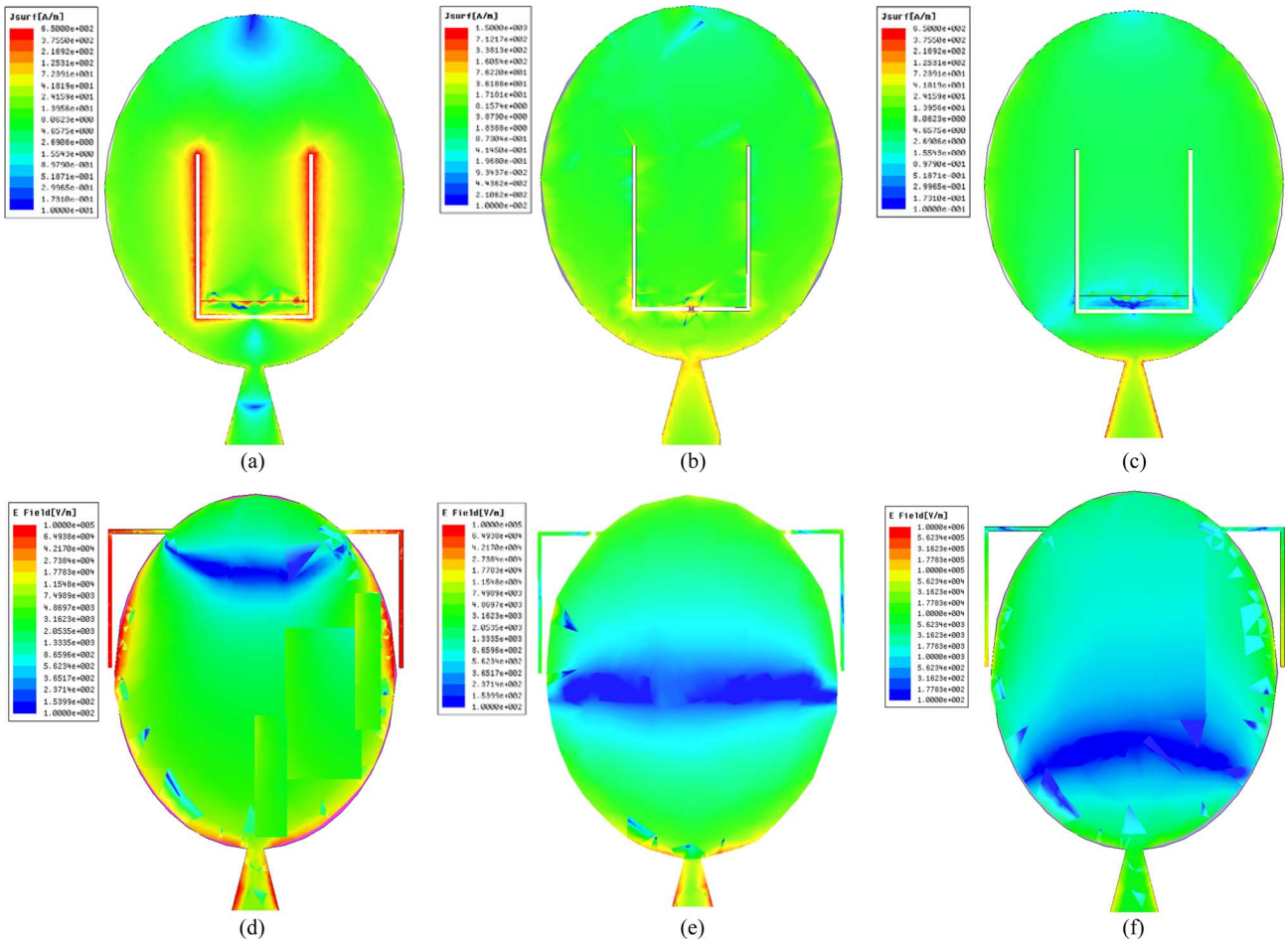

Fig. 3. Field distribution (a) open slot at 5.8 GHz, (b) shorted slot at 5.8 GHz, (c) open slot at 8 GHz, (d) shorted stubs at 5.8 GHz, (e) open stubs at 5.8 GHz, (f) shorted stubs at 8 GHz.

III. Operation Principles

For both antennas, the reconfigurability relies on the same concept of adding or removing a resonating structure. For the U-shaped slot antenna, the total length of the slot is approximately $\lambda/2$ at the frequency at which the rejection band is desired if the MEMS switch is up or open, and the MEMS switch shorts the slot at the center, which eliminates the resonance around 5 GHz. For the open stubs antenna, the two L-shaped, open circuit terminated stubs have a length approximately $\lambda/4$ at 5.8 GHz resulting in resonating elements that prevent radiation if the MEMS switches are down or closed, which connects the stub to the monopole.

A. Theory

The U-shaped slot resonates and therefore creates a band notch at the frequency that is related to its geometry dimensions as defined by: $f_U \sim (c/4(L_{S1} + (W_{S1}/2) - G_{S1}))$ where c is the speed of light [19]. The surface current distribution presented in Fig. 3(a) shows how the U-shaped slot resonates at 5.8 GHz and how this behavior is cancelled when the slot is shorted [Fig. 3(b), or at a different frequency (8 GHz current distribution is presented in Fig. 3(c)]. The directions of the current in the inner and outer side of the slot are opposite and they cancel each other as explained in detail in [14], [19]. As a result, the antenna does not radiate at that frequency and a frequency notch is created around the frequency of 5.8 GHz. When the slot is shorted at its center point by the MEMS switch, the total length of the slot is divided in two and, consequently, it cannot support the resonating currents; thus, radiation occurs as if the slot was not present. A simple transmission line model, similar to the approach introduced in [19], is presented in Fig. 4 that explains the slot effect. The presence of the slot is modeled as a $\lambda/4$ long, short circuit terminated series stub, which is similar to a spurline filter. The MEMS switch is across the input to the series stub. If the switch is up, [Fig. 4(a)] the spurline filter is in the circuit, and at the stub resonant frequency, there is an equivalent series open circuit that reflects the signal. However, if the switch is down, the spurline filter is shorted [Fig. 4(b)], or not in the circuit. Thus, radiation occurs at all frequencies.

Similarly the inverted L-shaped, open circuit terminated stubs resonate approximately at a frequency defined by: $f_{\text{inverted\_}L} \sim (c/4(W_{S2} + L_{S2}))$ where again c is the speed of light. Fig. 3(d) shows how the two stubs resonate at 5.8 GHz. When the two stubs are not connected to the elliptical radiator no currents flow through the stubs [Fig. 3(e)] but even when they are connected

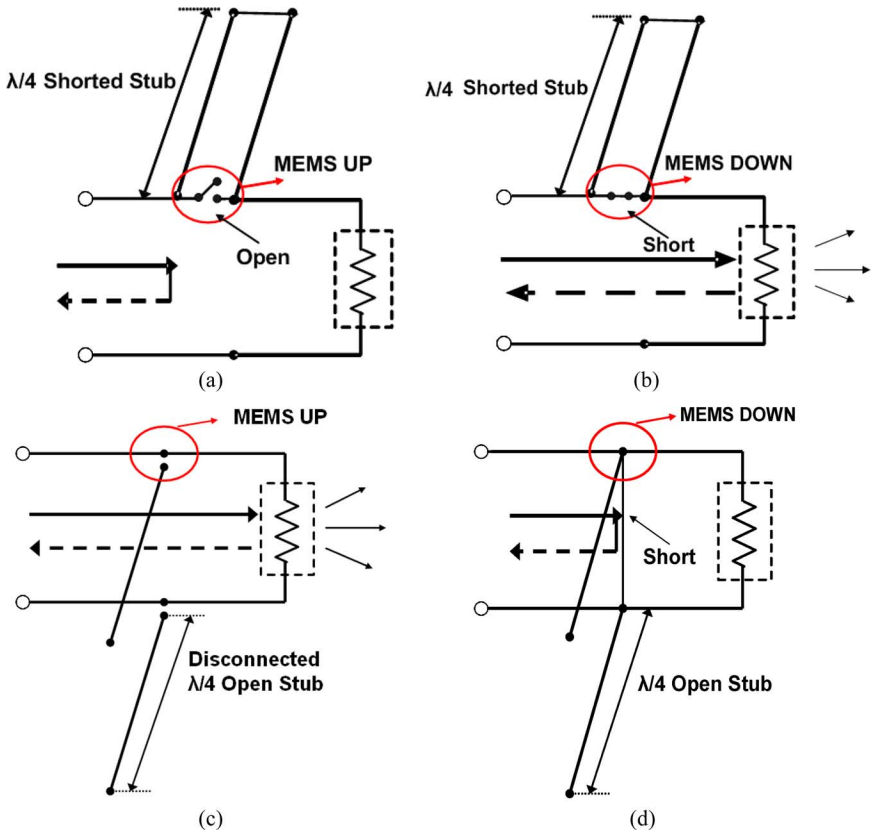

Fig. 4. Transmission line model for (a) U-shaped slot with MEMS up, (b) U shaped slot with MEMS down, (c) inverted L stubs with MEMS up, (d) inverted L stubs with MEMS down.

they do not resonate at a different frequency (8 GHz current distribution is presented in Fig. 3(f)). At the resonance frequency, the direction of the currents on the inverted L stub and the current along the nearby edge of the radiator are opposite to each other as presented in [20]. Therefore they cancel and the antenna does not radiate. Again a transmission line model is used to interpret the inverted L stubs effect on the radiation mechanism, where the presence of the two stubs is modeled as a $\lambda/4$ long stub. When the MEMS are in the "up" position, the stub is disconnected from the primary transmission line [Fig. 4(c)] and it has no effect on the incident power, which is radiated from the load ("antenna"). When the MEMS are in the "down" position the open stub appears as ideal short on the transmission line and the incident power is reflected as appears in Fig. 4(d).

B. Parametric Study

There is an inverse proportional relationship between the frequency of the band notch and the total length of the resonating elements as can be deduced from the approximate formulas presented in the previous section. This trend is verified numerically from the simulations presented in Fig. 5. Fig. 5(a) shows the simulation results when $\mathrm{L_{S1}}$ varies for an antenna with a U-shaped slot when the additional thin slot (3 μm wide) is not present. This example is referred to as "Simple Slot". When it is compared with the antenna that uses the additional thin slot (similar to the schematic in Fig. 1) to create the isolated floating ground, which is referred to as "Thin Slot", it can be seen that longer length $\mathrm{L_{S1}}$ is required to have the frequency notch between 5 and 6 GHz [Fig. 5(b)] when the thin slot is present. Specifically for the "Simple Slot," $\mathrm{L_{S1}} = 8.5$ mm is required for a stopband at 5.8 GHz, whereas for the "Thin Slot," a little longer length of $\mathrm{L_{S1}} = 8.8$ is needed to cause a band notch in the same frequency range. Additionally, when the same length $\mathrm{L_{S1}} = 8.5$ is used for "Thin Slot", the band notch shifts higher to approximately 6.0 GHz as can be seen in Fig. 5(b). Similar behavior is observed for the length of the inverted L stubs, which is presented in Fig. 5(c). The longer the length $\mathrm{L_{S2}}$ is, the lower the frequency of the band notch shifts. In each of the above simulations, all of the other dimensions are kept constant.

Simulations show that another important parameter is the position of the resonating element, especially for the U-shaped slot. Fig. 6 shows the simulated reflection coefficient for the two antennas as a function of the resonating element location. Fig. 6(a) shows that the stopband frequency varies by 1.5 GHz if $\mathrm{D_1}$ is varied by 1 mm. Furthermore, the magnitude of the reflection coefficient is seen to be dependent on the slot position, with a smaller reflection if $\mathrm{D_1}$ is large. The large dependence on slot position is due to the strong currents at the elliptical radiator feed point, which couple strongly to the U-shaped slot. On the contrary, a small variation on the distance $\mathrm{D_2}$ of the two L-shaped stubs from the top point of the ellipse does not seem to affect the band notch significantly. Fig. 6(b) shows that a 1 mm variation in stub location only causes a 750 MHz variation in stopband frequency. It is also noted that the magnitude of the

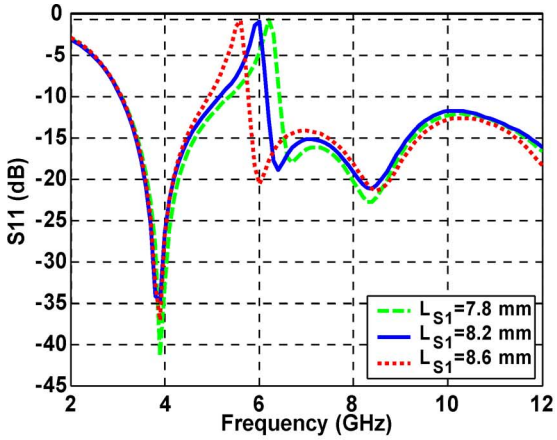

(a)

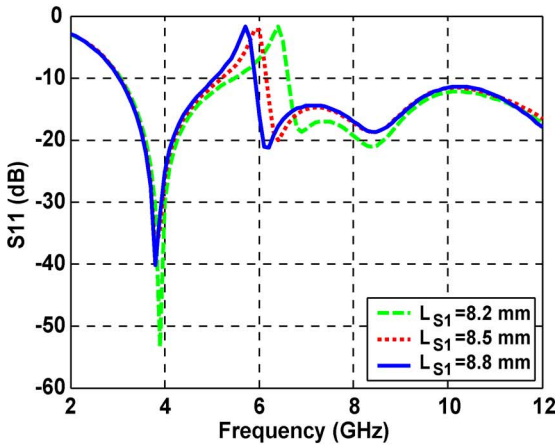

(b)

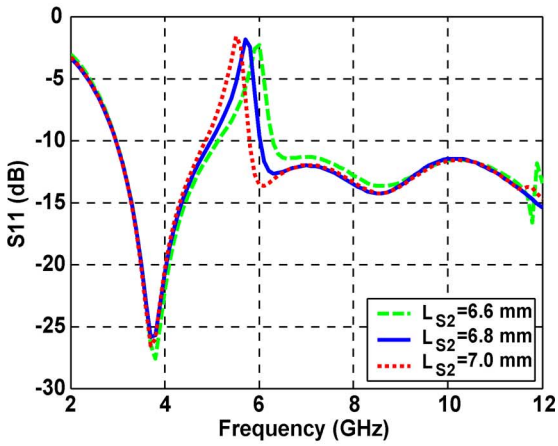

(c)

Fig. 5. Slot/stub length effect on return loss (a) simple slot, (b) thin slot, (c) stubs.

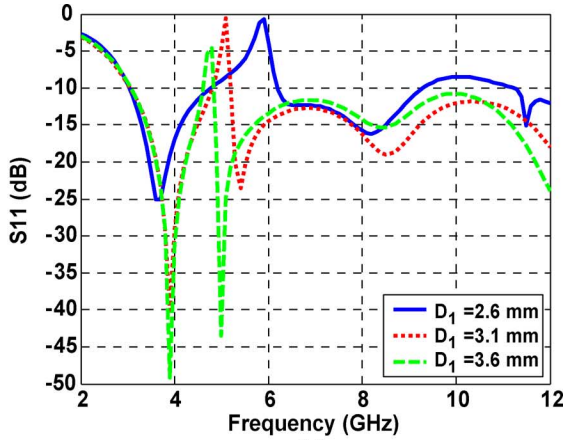

(a)

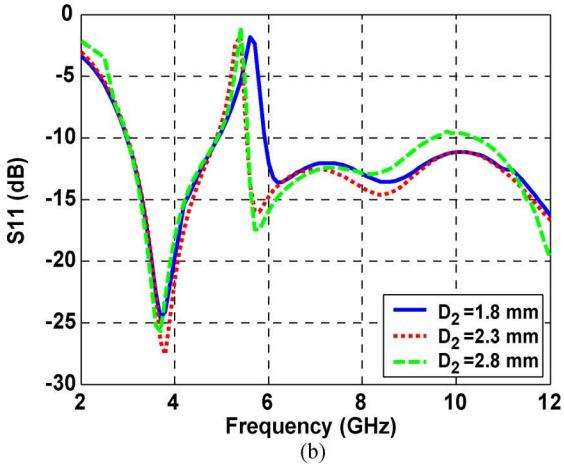

(b)

Fig. 6. (a) Slot position effect, (b) stub position effect.

reflection coefficient does not appear to be dependent on the stub location.

IV. MEMS Switches Operation and Integration

A. MEMS Switch Operation

MEMS switches were chosen for this application because of their low loss, excellent isolation, and wide-band response. The challenge with any switch integration in an antenna system is with biasing the switches without affecting the radiation characteristics. To avoid this issue, the biasing technique recently introduced in [21] was implemented. The major advantage of the suggested MEMS switches is that they do not require dc bias lines in order to be actuated. For this technique to work, there must be a dc short between the signal line input (center pin on the CPW antenna feed) and the posts of the MEMS switches. This method also requires that the MEMS are Ohmic and single-supported.

The dc actuation voltage is applied directly to the CPW center pin through a dc bias on the vector network analyzer. When no voltage is applied, the switches are in the up position and the antenna exhibits one behavior. When a voltage is applied, an electrostatic force pulls down the MEMS switches and since they are Ohmic, they create a dc and RF short at the contact point. The antenna now exhibits a different behavior.

Since there is a dc short between the signal line input and the posts of the MEMS switches, no additional metal lines are required to apply the actuation voltage. To avoid the addition of dc ground lines, a floating ground is used. In this method, a metal pad beneath the switch is not shorted to anything. It does not represent a true ground, but it is sufficient to provide a foundation for electrostatic force generation. The pad is isolated from direct contact with the switch membrane by a thin layer of silicon

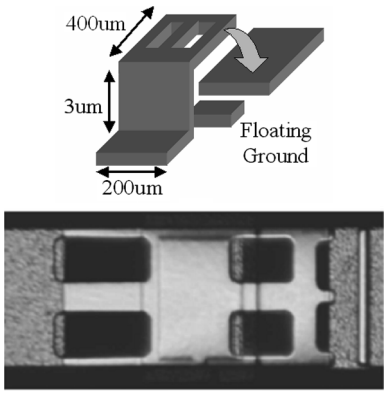

Fig. 7. (a) The MEMS switch geometry and floating ground concept are shown. (b) The fabricated MEMS switch is shown. The post is located on the left and the ohmic contact is made on the right.

nitride. To avoid failures due to dielectric charging, this method should only be used in systems that will be continuously reconfigured. The details of this biasing method are described further in [21]. The MEMS switch geometry is shown in Fig. 7(a). and the fabricated switch is presented in Fig. 7(b).

V. Measurements Discussion

A. Return Loss Measurements

For the return loss measurements, an Agilent 8510 vector network analyzer was used and the input signal was launched through 850 μm pitch ground-signal-ground probes. The probes were preferred over coaxial connectors because they allow the direct application of the dc voltage. The dc voltage for the MEMS actuation was applied through the RF cable that connects to the network analyzer and it follows the same path with the RF signal. An S_{11} measurement was taken when the MEMS were "up" (OFF state) without applying any dc voltage and another measurement was taken when 28 V dc voltage was applied and the MEMS' bridge went down, switching to ON state. The return loss measurements are compared with the "Reference" antenna, which is a sample without any resonating elements. The measured S_{11} plots [Fig. 8(a)] for the "Reference" antenna and the U-shaped slot antenna when the MEMS membrane is down (MEMS Down) are in very good agreement; when the switch membrane is in "up" position (MEMS Up) a frequency notch appears between 5 and 6 GHz. In Fig. 8(b) the same results are presented for the antenna with the inverted L stubs. The only difference is that the band notch appears when the switch is in "down" position (MEMS Down) and the "Reference" antenna has similar return loss behavior with the antenna with the switch not actuated (MEMS Up). The presented return loss measurements verify the good performance of the MEMS switches and the effectiveness of the suggested integration. The simulated radiation efficiency was higher than 85% in all cases and it was not significantly affected by the presence of neither the stubs nor the slot.

B. Radiation Pattern Measurements

The radiation patterns are measured on an antenna probe station measurement system that permits 360 degree of rotation

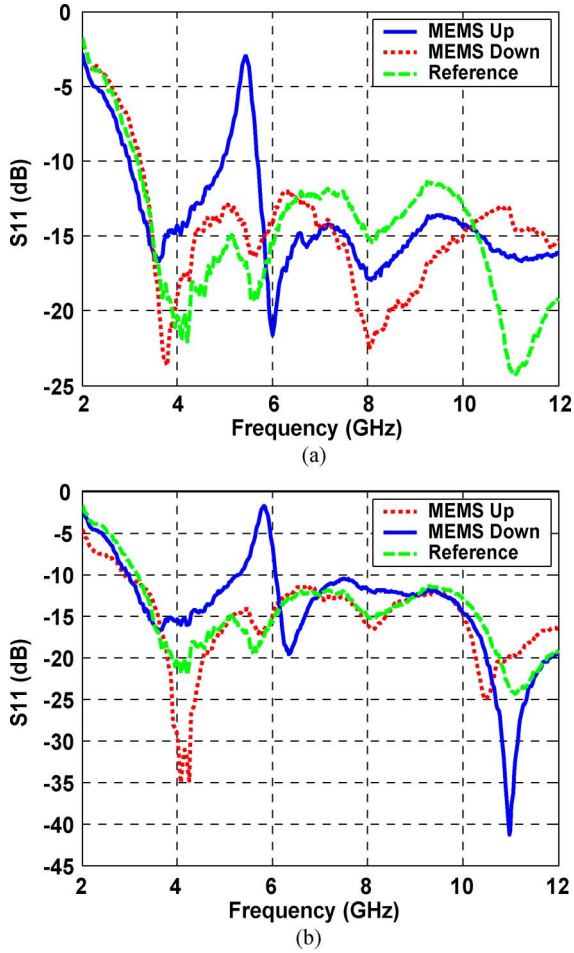

Fig. 8. (a) Return loss for antenna with MEMS reconfigurable slot, (b) return loss for antenna with MEMS reconfigurable stubs.

with 850 mm pitch probes. However, even with a specially made probe with an extended microcoax section, the probe positioner and probe itself cause interference with the radiated fields. Therefore, only parts of the measured field patterns are shown. Measurements at 5.8 and 8 GHz are presented in both E (x-y) and H (x-z) planes. Fig. 9 shows the radiation patterns for the U-shaped slot antenna and Fig. 10 demonstrates the radiation patterns for the L-shaped stubs antenna. The two states (shorted and open, which correspond to ON and OFF states of a MEMS switch) of the reconfigurable antennas are compared with the "Reference" antenna. It is seen (radiation patterns at 8 GHz) that the addition of the resonating elements does not significantly affect the radiation performance of the antennas in frequencies outside the 5–6 GHz range. On the other hand within the band-notch range (radiation patterns at 5.8 GHz) and with the appropriate MEMS switch state the radiated field intensity is degraded [Fig. 9(a) and (c), Fig. 10(a) and (c)]. The radiated field degradation in the band-notch range is also verified from the gain measurements shown in Fig. 11.

C. Gain Measurements

The antenna gain was measured by using the substitution method. For the "known" antennas, open ended rectangular waveguides are used with the gain of them determined by

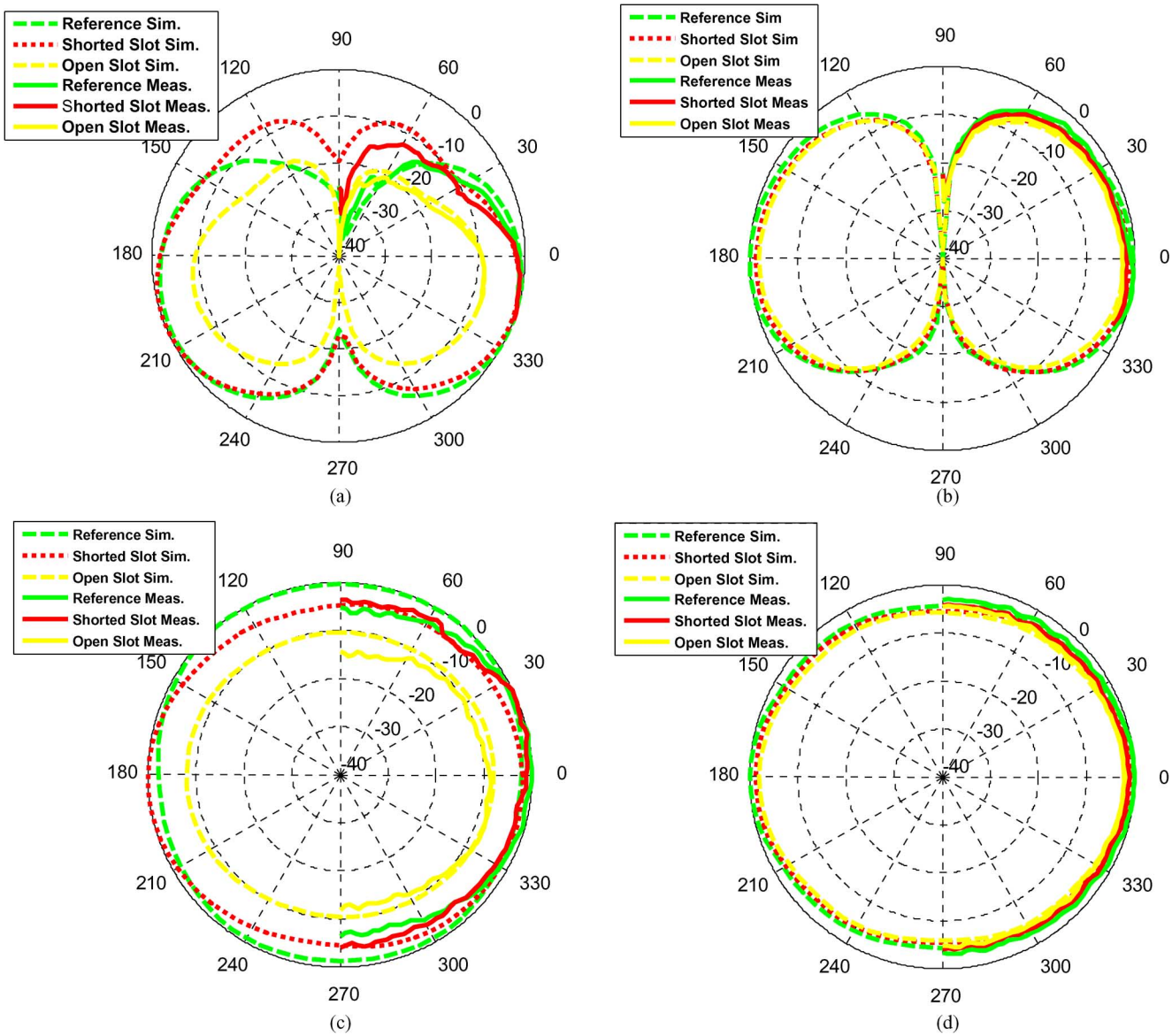

Fig. 9. U-shaped slot radiation pattern measurements and simulations, (a) E plane at 5.8 GHz (b) E plane at 8 GHz, (c) H plane at 5.8 GHz (d) H plane at 8 GHz.

[22]. The gain measurements shown in Fig. 11 were taken in the directivity direction which coincides with the z axis direction as it is defined in Fig. 1. As can be seen, the presence of the resonating elements and the frequency mismatch cause a significant degradation on the gain value at the frequency band to be rejected in a reconfiguring way. The antenna gain is suppressed by over 10 dB for the slot resonator and 6 dB for the stub resonator. The gain behavior over the remainder of the frequency band is similar for all three cases as can be verified from Fig 11.

VI. Conclusion

The use of resonating elements integrated with MEMS switches has been exploited to implement two UWB monopoles with reconfigurable band notch in the wireless LAN frequency range (5.150–5.825 GHz). The basic antenna design is an elliptical radiator fed with CPW line, fabricated on thin organic material. In the first case a U-shaped slot of approximate length $\lambda/2$ causes the frequency notch and its effect can be dynamically cancelled by a MEMS switch that shorts the slot. The antenna with the shorted slot has the same response with an antenna without any slot, and consequently the state of the single switch defines the presence or not of the rejection band. In the second case, two inverted L-shaped open stubs are used and two MEMS switches are used to connect and disconnect the stubs with the elliptical radiator. The electrical connection of the stubs with the radiator causes the creation of the rejection band and, apparently, when the stubs are not electrically connected, the antenna operates as a typical UWB radiator with radiation band that covers the whole UWB range (3.1–10.6 GHz). Reconfigurability is achieved with MEMS switches that are actuated through the RF signal path, without the need of dc bias lines, that could potentially complicate the switch fabrication and integration process, while degrading the radiation performance of any antenna and especially of a broadband antenna because RF leakage through the bias

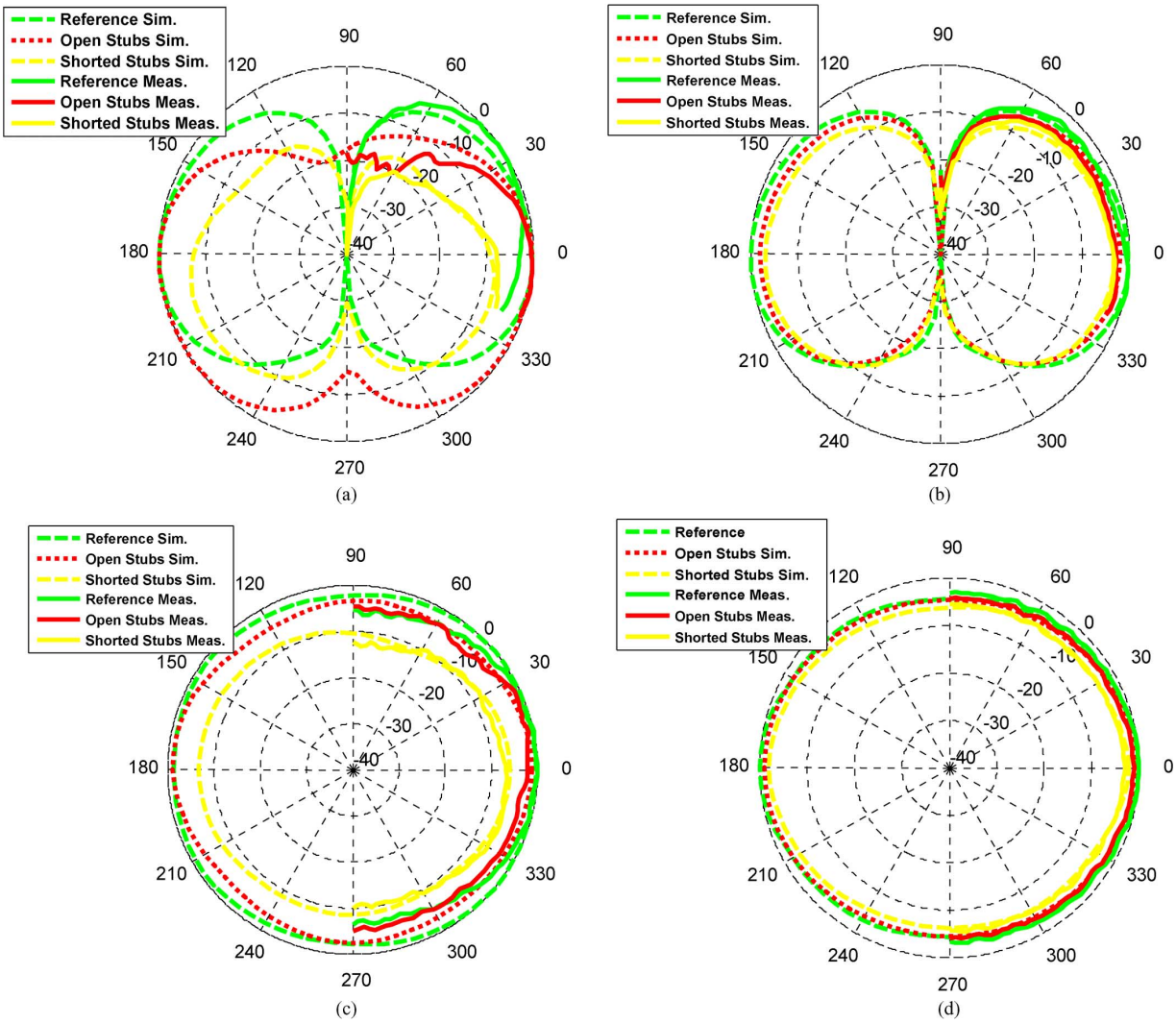

Fig. 10. L-shaped stubs radiation pattern measurements and simulations (a) E plane at 5.8 GHz, (b) E plane at 8 GHz, (c) H plane at 5.8 GHz, (d) H plane at 8 GHz.

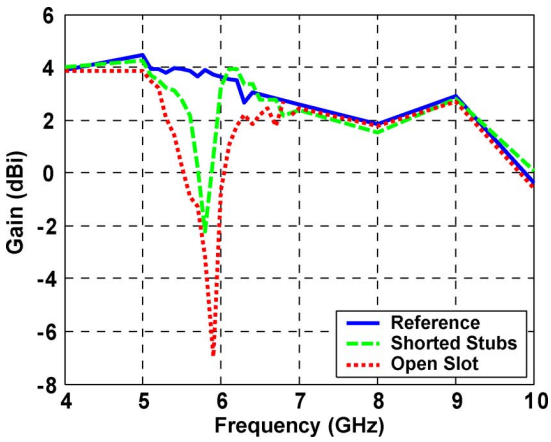

Fig. 11. Gain measurements.

lines cannot be avoided. Numerical results, transmission line models and eventually measurements verify the very satisfactory performance of the proposed antennas which can be good candidates for next generation, high performance and high versatility cognitive radios.

REFERENCES

[1] S. Haykin, "Cognitive radio: Brain-empowered wireless communications," *IEEE J. Select. Areas Comm.*, vol. 23, pp. 201–220, Feb. 2005.
[2] K.-H. Kim, Y.-J. Cho, S.-P. Hwang, and S.-O. Park, "Band-notched UWB planar monopole antenna with two parasitic patches," *Electron. Lett.*, vol. 41, no. 14, pp. 783–785, Jul. 7, 2005.
[3] I.-J. Yoon, H. Kim, and Y. J. Yoon, "UWB RF receiver front-end with band-notch characteristic of 5 GHz WLAN," in *IEEE Int. Antenna Propag. Symp. Digest*, Jul. 2006, pp. 1303–1306.
[4] S.-Y. Chen, P.-H. Wang, and P. Hsu, "Uniplanar log-periodic slot antenna fed by a CPW for UWB applications," *IEEE Antenna Wireless Propag. Lett.*, vol. 5, no. 1, pp. 256–259, Dec. 2006.
[5] J. Kim, C. S. Cho, and J. W. Lee, "5.2 GHz notched ultra-wideband antenna using slot-type SRR," *Electron. Lett.*, vol. 42, no. 6, pp. 315–316, Mar. 16, 2006.
[6] K. Chang, H. Kim, and Y. J. Yoon, "Multi-resonance UWB antenna with improved band notch characteristics," in *IEEE Int. Antenna Propag. Symp. Digest*, Jul. 2005, vol. 3A, pp. 516–519.
[7] S.-W. Qu, J.-L. Li, and Q. Xue, "A band-notched ultrawideband printed monopole antenna," *IEEE Antenna Wireless Propag. Lett.*, vol. 5, no. 1, pp. 495–498, Dec. 2006.

[8] S.-Y. Suh, W. L. Stutzman, W. A. Davis, A. E. Waltho, K. W. Skeba, and J. L. Schiffer, "A UWB antenna with a stop-band notch in the 5-GHz WLAN band," in *Proc. IEEE ACES*, Apr. 2005, pp. 203–207.
[9] W. J. Lui, C. H. Cheng, and H. B. Zhu, "Compact frequency notched ultra-wideband fractal printed slot antenna," *IEEE Microw. Wireless Comp. Lett.*, vol. 16, no. 4, pp. 224–226, Apr. 2006.
[10] W. J. Lui, C. H. Cheng, and H. B. Zhu, "Frequency notched printed slot antenna with parasitic open-circuit stub," *Electron. Lett.*, vol. 41, no. 20, pp. 1094–1095, Sep. 29, 2005.
[11] T. Dissanayake and K. P. Esselle, "Design of slot loaded band-notched UWB antennas," in *IEEE Int. Antenna Propag. Symp. Digest*, Jul. 2005, vol. 1B, pp. 545–548.
[12] A. J. Kerkhoff and L. Hao, "Design of a band-notched planar monopole antenna using genetic algorithm optimization," *IEEE Trans. Antennas Propag.*, vol. 55, no. 3, pt. 1, pp. 604–610, Mar. 2007.
[13] K. Chung, J. Kim, and J. Choi, "Wideband microstrip-fed monopole antenna having frequency band-notch function," *IEEE Microw. Wireless Comp. Lett.*, vol. 15, no. 11, pp. 766–768, Nov. 2005.
[14] Y. J. Cho, K. H. Kim, D. H. Choi, S. S. Lee, and S.-O. Park, "A miniature UWB planar monopole antenna with 5-GHz band-rejection filter and the time-domain characteristics," *IEEE Trans. Antennas Propag.*, vol. 54, no. 5, pp. 1453–1460, May 2006.
[15] Y.-C. Lin and K.-J. Hung, "Compact ultrawideband rectangular aperture antenna and band-notched designs," *IEEE Trans. Antennas Propag.*, vol. 54, no. 11, pt. 1, pp. 3075–3081, Nov. 2006.
[16] D. E. Anagnostou, G. Zheng, M. T. Chryssomallis, J. C. Lyke, G. E. Ponchak, J. Papapolymerou, and C. G. Christodoulou, "Design, fabrication, and measurements of an RF-MEMS-based self-similar reconfigurable antenna," *IEEE Trans. Antennas Propag.*, vol. 54, no. 2, pt. 1, pp. 422–432, Feb. 2006, J..
[17] A. C. K. Mak, C. R. Rowell, R. D. Murch, and C. L. Mak, "Reconfigurable multiband antenna designs for wireless communication devices," *IEEE Trans. Antennas Propag.*, vol. 55, no. 7, pp. 1919–1928, Jul. 2007.
[18] C. W. Jung, M.-J. Lee, G. P. Li, and F. De Flaviis, "Reconfigurable scan-beam single-arm spiral antenna integrated with RF-MEMS switches," *IEEE Trans. Antennas Propag.*, vol. 54, no. 2, pt. 1, pp. 455–463, Feb. 2006.
[19] W.-S. Lee, D.-Z. Kim, K.-J. Kim, and J. W. Yu, "Wideband planar monopole antennas with dual band-notched characteristics," *IEEE Trans. Microw. Theory Tech.*, vol. 54, no. 6, pt. 2, pp. 2800–2806, Jun. 2006.
[20] B. Kim, S. Nikolaou, D. E. Anagnostou, Y. S. Kim, M. M. Tentzeris, and J. Papapolymerou, "A conformal L-shaped antenna on liquid crystal polymer substrate for ultra-wideband systems with WLAN band-stop characteristics," *IEEE Trans. Antennas Propag.*, submitted for publication.
[21] N. Kingsley, D. E. Anagnostou, M. M. Tentzeris, and J. Papapolymerou, "RF MEMS sequentially-reconfigurable Sierpinski antenna on a flexible, organic substrate without the need for dc bias lines," *IEEE Trans. Antennas Propag.*, submitted for publication.
[22] A. D. Yaghjian, "Approximate formulas for the far field and gain of open-ended rectangular waveguide," *IEEE Trans. Antennas Propag.*, vol. AP-32, no. 4, pp. 378–384, Apr. 1984.

Symeon (Simos) Nikolaou (M'08) received the B.S.E.C.E. degree from the National Technical University of Greece (NTUA) Athens, Greece, in 2003 and the M.S.E.C.E. and Ph.D. degrees from the Georgia Institute of Technology (GaTech), Atlanta, in 2005 and 2007, respectively.

Since September 2007, he has been a Lecturer at Frederick University, Nicosia Cyprus. He has authored or coauthored more than 25 publications in peer reviewed journals and conferences. His research interests include the design of UWB, conformal and reconfigurable antennas, compact RFIDs and reconfigurable filters on organic materials.

Nickolas D. Kingsley (M'07) received the Ph.D. degree from the Georgia Institute of Technology, Atlanta, in May 2007.

His research interests included the design, miniaturization, fabrication, packaging, and testing of RF MEMS multilayer front ends. During his Ph.D. studies, he focused on novel technologies using liquid crystal polymer (LCP) substrate. He has filed four invention disclosures related to LCP innovations, has published over a dozen papers in peer reviewed journals and conferences, and has a published book chapter on RF MEMS devices. He joined Auriga Measurement Systems, Lowell, MA, in June 2007 as a Principal Engineer in the Measurement, Modeling, and Design Group. He is currently working on ultrahigh efficiency power amplifier and module designs.

Dr. Kingsley is a member of the IEEE Antennas and Propagation Society, the IEEE Microwave Theory and Techniques Society, and the Order of the Engineer. He is serving on the 2009 International Microwave Symposium Steering Committee and Technical Program Committee.

George E. Ponchak (S'82–M'83–SM'97–F'08) received the B.E.E. degree from Cleveland State University, Cleveland, OH, in 1983, the M.S.E.E. degree from Case Western Reserve University, Cleveland, OH, in 1987, and the Ph.D. in electrical engineering from the University of Michigan, Ann Arbor, in 1997.

He joined the staff of the Communication Technology Division at NASA Glenn Research Center, Cleveland, in 1983 where he is now a Senior Research Engineer. In 1997–1998 and in 2000–2001, he was a Visiting Professor at Case Western Reserve University. He has authored and coauthored over 150 papers in refereed journals and symposia proceedings. His research interests include the development and characterization of microwave and millimeter-wave printed transmission lines and passive circuits, multilayer interconnects, uniplanar circuits, Si and SiC radio frequency integrated circuits, and microwave packaging.

Dr. Ponchak is a Fellow of the IEEE and an Associate Member of the European Microwave Association. Dr. Ponchak is Editor-in-Chief of the IEEE MICROWAVE AND WIRELESS COMPONENTS LETTERS, and he was Editor of a special issue of the IEEE TRANSACTIONS ON MICROWAVE THEORY AND TECHNIQUES on Si MMICs. He founded the IEEE Topical Meeting on Silicon Monolithic Integrated Circuits in RF Systems and served as its Chair in 1998, 2001, and 2006. He served as Chair of the Cleveland MTT-S/AP-S Chapter (2004–2006), and he has chaired many symposium workshops and special sessions. He is a member of the IEEE International Microwave Symposium Technical Program Committee on Transmission Line Elements and served as its Chair in 2003–2005 and a member of the IEEE MTT-S Technical Committee 12 on Microwave and Millimeter-Wave Packaging and Manufacturing. He served on the IEEE MTT-S AdCom Membership Services Committee (2003–2005). He received the Best Paper of the ISHM'97 30th International Symposium on Microelectronics Award.

John Papapolymerou (S'90–M'99–SM'04) received the B.S.E.E. degree from the National Technical University of Athens, Athens, Greece, in 1993 and the M.S.E.E. and Ph.D. degrees from the University of Michigan, Ann Arbor, in 1994 and 1999, respectively.

From 1999–2001 he was an Assistant Professor at the Department of Electrical and Computer Engineering, University of Arizona, Tucson. In 2001, he joined the School of Electrical and Computer Engineering, Georgia Institute of Technology, where he is currently an Associate Professor. He has authored or coauthored over 240 publications in peer reviewed journals and conferences. His research interests include the implementation of micromachining techniques and MEMS devices in microwave, millimeter-wave and THz circuits and the development of both passive and active planar circuits on semiconductor (Si/SiGe, GaAs) and organic substrates (LCP, LTCC) for System-on-a-Chip (SOC)/System-on-a-Package (SOP) RF front ends.

Dr. Papapolymerou is the Chair for Commission D of the US National Committee of URSI and currently serves as an Associate Editor for

IEEE MICROWAVE AND WIRELESS COMPONENT LETTERS and the IEEE TRANSACTIONS ON ANTENNAS AND PROPAGATION. During 2004 he was the Chair of the IEEE MTT/AP Atlanta Chapter. He was the recipient of the 2004 Army Research Office (ARO) Young Investigator Award, the 2002 National Science Foundation (NSF) CAREER award, the best paper award at the 3rd IEEE International Conference on Microwave and Millimeter-Wave Technology (ICMMT2002), Beijing, China and the 1997 Outstanding Graduate Student Instructional Assistant Award presented by the American Society for Engineering Education (ASEE), The University of Michigan Chapter. His students have also been recipients of several awards including the Best Student Paper award of the 2004 IEEE Topical Meeting on Silicon Monolithic Integrated Circuits in RF Systems, the 2007 IEEE MTT graduate fellowship and the 2007–2008 IEEE MTT undergraduate scholarship/fellowship.

Manos M. Tentzeris received the Diploma Degree (*magna cum laude*) in electrical and computer engineering from the National Technical University of Athens, Athens, Greece and the M.S. and Ph.D. degrees in electrical engineering and computer science from the University of Michigan, Ann Arbor, MI.

He is currently an Associate Professor with School of Electrical and Computer Engineering, Georgia Tech, Atlanta. He has published more than 310 papers in refereed journals and conference proceedings, three books and 15 book chapters. He has helped develop academic programs in highly integrated/multilayer packaging for RF and wireless applications using ceramic and organic flexible materials, paper-based RFIDs, power scavengers and sensors, Microwave MEM's, SOP-integrated (UWB, multiband, conformal) antennas and Adaptive Numerical Electromagnetics (FDTD, multiresolution algorithms) and heads the ATHENA research group (20 researchers). He is the Georgia Electronic Design Center Associate Director for RFID/sensors research, and he has been the Georgia Tech NSF-Packaging Research Center Associate Director for RF research and the RF Alliance Leader from 2003–2006. He is also the leader of the RFID Research Group of the Georgia Electronic Design Center (GEDC) of the State of Georgia. He was a Visiting Professor with the Technical University of Munich, Germany for summer 2002, where he introduced a course in the area of high-frequency packaging.

Prof. Tentzeris is a member of URSI Commission D, a member of MTT-15 committee, an Associate Member of EuMA, a Fellow of the Electromagnetic Academy and a member of the Technical Chamber of Greece. He was the recipient/co-recipient of the 2007 IEEE APS Symposium Best Student Paper Award, the 2007 IEEE IMS Third Best Student Paper Award, the 2007 ISAP 2007 Poster Presentation Award, the 2006 IEEE MTT Outstanding Young Engineer Award, the 2006 Asian-Pacific Microwave Conference Award, the 2004 IEEE TRANSACTIONS ON ADVANCED PACKAGING Commendable Paper Award, the 2003 NASA Godfrey "Art" Anzic Collaborative Distinguished Publication Award, the 2003 IBC International Educator of the Year Award, the 2003 IEEE CPMT Outstanding Young Engineer Award, the 2002 International Conference on Microwave and Millimeter-Wave Technology Best Paper Award (Beijing, China), the 2002 Georgia Tech-ECE Outstanding Junior Faculty Award, the 2001 ACES Conference Best Paper Award and the 2000 NSF CAREER Award and the 1997 Best Paper Award of the International Hybrid Microelectronics and Packaging Society. He was the TPC Chair for IEEE IMS 2008 Symposium and the Chair of the 2005 IEEE CEM-TD Workshop and he is the Vice-Chair of the RF Technical Committee (TC16) of the IEEE CPMT Society. He has organized various sessions and workshops on RF/Wireless Packaging and Integration, RFID's, Numerical Techniques/Wavelets, in IEEE ECTC, IMS, VTC and APS Symposia in all of which he is a member of the Technical Program Committee in the area of "Components and RF." He is the Associate Editor of the IEEE TRANSACTIONS ON MICROWAVE THEORY AND TECHNIQUES, IEEE TRANSACTIONS ON ADVANCED PACKAGING and the *International Journal on Antennas and Propagation*. He has given more than 50 invited talks in the same area to various universities and companies in Europe, Asia and America.